



RSC Advances

Self-Healing Composite Hydrogel with Antibacterial and Reversible Restorability Conductive Properties

Journal:	<i>RSC Advances</i>
Manuscript ID	RA-ART-01-2020-000089.R1
Article Type:	Paper
Date Submitted by the Author:	24-Jan-2020
Complete List of Authors:	Ginting, Mimpin; Universitas Sumatera Utara, Chemistry Pasaribu, Subur; Mulawarman University, Department of Chemistry Masmur, Indra; Universitas Sumatera Utara, Chemistry Kaban, Jamaran; Universitas Sumatera Utara, Department of Chemistry Hestina, Hestina; Universitas Sari Mutiara, Department of Chemistry
Subject area & keyword:	Gels & soft matter < Materials

SCHOLARONE™
Manuscripts

RSC Advances

Guidelines for Reviewers

Thank you very much for agreeing to review this manuscript for [RSC Advances](#).



RSC Advances is the largest gold open access journal dedicated to the chemical sciences. We are here for everyone who wants to publish quality chemistry research and share it with the world.

RSC Advances publishes work in all areas of chemistry and reaches a global readership, and our low APCs, discounts and waivers make publishing open access achievable and sustainable.

RSC Advances' Impact Factor is **3.049** (2018 Journal Citation Reports®)

The following manuscript has been submitted for consideration as a

FULL PAPER

To be suitable for publication in *RSC Advances*, all papers must contain some chemistry. The work must be high quality, well conducted and advance the development of the field.

It is essential that all research work reported in *RSC Advances* is well-carried out and well-characterised. There should be enough supporting evidence for the claims made in the manuscript. When making your recommendation please:

- comment on the originality and scientific reliability of the work;
- comment on the characterisation of the compounds/materials reported – has this been accurately interpreted and does it support the conclusions of the work?
- state clearly whether you would like to see the article accepted or rejected and give detailed comments that will both help the Editor to make a decision on the article and the authors to improve the article;

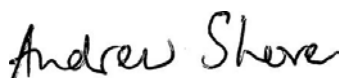
Please inform the Editor if:

- there is a conflict of interest
- there is a significant part of the work that you are not able to referee with confidence
- the work, or a significant part of the work, has previously been published
- the work represents part of an unduly fragmented investigation

Best regards,



Professor Russell Cox
Editor-in-Chief
Leibniz Universität Hannover



Dr Andrew Shore
Executive Editor
Royal Society of Chemistry

Contact us

Please visit our [reviewer hub](#) for further details of our processes, policies and reviewer responsibilities as well as guidance on how to review, or click the links below.



What to do
when you
review



Reviewer
responsibilities



Process &
policies

Dear Dr. Juan J. Giner-Casares

We would like to thank the editor for very careful review and for the constructive suggestions on our manuscript. We also appreciate the time and efforts by the editor and reviewers in reviewing this manuscript. We have adopted the suggestions and the appropriate changes have been introduced to the main text of the revised manuscript (highlighted in yellow). Moreover, we also added more information in each analyses (including their figures) in the results and discussion part. Therefore, we hope that you find our responses satisfactory and that the revised manuscript is now completely acceptable for publication in RSC Advances.

We look forward to receive further communications.

Sincerely,
Mimpin Ginting

We would like to thank the reviewer for careful and thorough reading of this manuscript and for the thoughtful comments and suggestions. Comments and Responses to your comments are given below.

Response to Reviewer #1:

The manuscript reports a facile method to fabricate PAA/Ppy-Fe hydrogel with self-healing, antibacterial and conductive properties via free-radical polymerization. The exist of Ppy and Fe³⁺ provides good antibacterial property. The antibacterial property is examined on escherichia coli via the disk diffusion method. In addition, the demonstration of the electrical conductivity application is interesting. However, there are some issues needed to be addressed:

1. To better analyze the influences of adding Ppy, it is better to increase a control group that only exists PAA and Fe³⁺ without Ppy.

Response: Thanks for the thoughtful comments and suggestions. In the revised manuscript, we have prepared the PAA-Fe³⁺ hydrogels without Ppy as the control group including their analyses. The concentrations of acrylic acid and Fe³⁺ are 30 w/v% and 0.5 mol% of AA, respectively.

2. The manuscript lacks the effect of Fe³⁺ concentration on hydrogel properties, thus the relevant experiments need to be completed.

Response: Thanks for drawing our attention to this study. Regarding this comment, we conducted the experiments by varying Fe³⁺ concentration in the hydrogels and carried out the analyses as well. As the experiment, we varied the concentration of Fe³⁺ from 0.1 to 0.3, 0.5, 0.7 and 1 mol% of AA followed by the characterization of swelling degree, gel fraction, and mechanical properties on the resulted hydrogels.

3. In order to better demonstrate the self-healing properties of the hydrogels and to obtain an accurate self-healing time, there need SEM images of the self-healing process.

Response: Thanks for the comment. To address this issue, we have performed the SEM analysis of hydrogels during the self-healing processes. As in the revised manuscript, SEM images of the self-healing processes was shown in Fig. 1S in Electronic Supplementary Information (ESI).

4. The causality of the sentence “Apart from that, at higher cross-linking density, the migration of ions in the hydrogels was hindered, thus the resistance decreases with increasing pyrrole concentration” is not clear.

Response: Thanks for the comment. For this sentence, we have made a mistake. In fact, we would like to describe that the resistance increase with increasing cross-linking density. Thus, we have revised it into “*Likewise, at higher cross-linking density, rigid network was obtained and lead to hindrance for ions migration in the hydrogel networks therefore caused the resistance increase*”

5. Additionally to the given references, there are some more recent references within this field, which could substitute some old ones or at least to be added:

Journal of Materials Chemistry B, 2019, 7, 5704-5712;

ACS Applied Materials & Interfaces, 2018, 10, 36218-36228.

Response: Thanks for the suggestion. We have added and cited the aforementioned references in the references of the revised manuscript. The conductivity properties of hydrogels in our works possessed similar results with both of the references in which as the pyrrole concentration increases, the conductivity of hydrogels increases.

6. There are several grammar errors, please revise carefully.

Response: Thanks for the constructive advice. Regarding the grammatically errors, we have tried our best for the grammar. Hence, we have re-read and tried to improve the grammar within the revised manuscript.

In summary, I recommend the acceptance of this manuscript after minor revisions noted above.

Response to Reviewer #2:

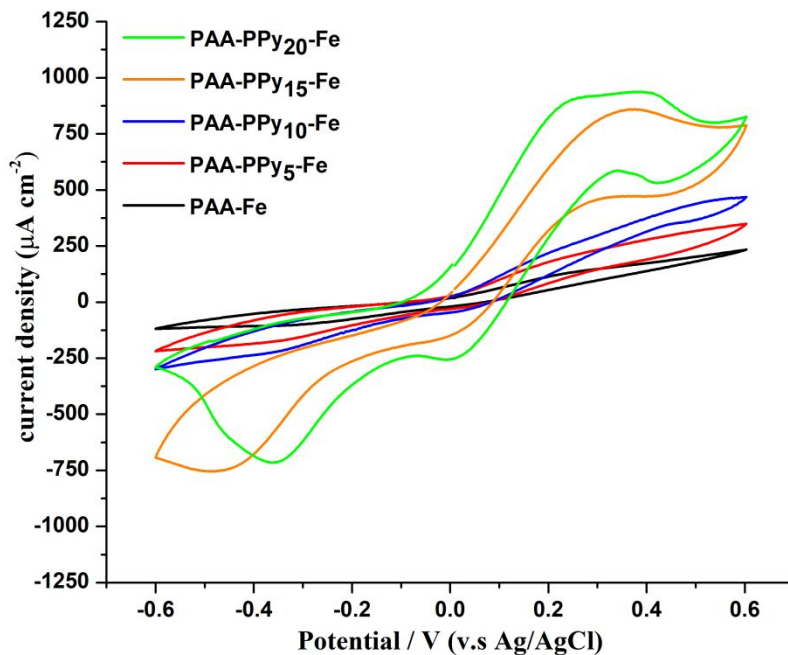
In this manuscript, the polymer hydrogels containing polyacrylic acid (PAA), Fe³⁺ and polypyrrole (PPy) were designed and synthesized. These hydrogels show good mechanical properties and self-healing properties. Moreover, the antibacterial activity as well as the electrical conductivity of these hydrogels were analyzed. Overall, multicomponent polymer hydrogels are promising soft materials. And the structures and properties of the hydrogels were thoroughly characterized. In principle, developing novel soft matters is a very important research topic. And the results showing in this manuscript could be useful for the design of multifunctional hydrogels. The studies have been done carefully and experimental description is sound. There are few points which the authors should consider.

1. For measuring electrical conductivity, what is the water content in the hydrogels? The results showing in Figure 8 suggest that the conductivity is dependent on the concentration of polypyrrole. However, the water content may also change the conductivity.

Response: Thanks for the insightful comment. Previously, we have measured and maintained the water content for all hydrogels which is fixed at 50%. Therefore, the study of conductivity (as shown in Fig. 8) with variation of pyrrole concentration can be investigated and that the effect of water content in the hydrogels can be neglected. We also have added the information regarding the water content of the hydrogels in the revised manuscript.

2. Please check the cyclic voltammetry of the hydrogels.

Response: Thanks for the suggestion. In fact, the CV study of such hydrogels has been conducted previously. Briefly, the CV analysis was performed using Electrochemical workstation (CHI 614D) in a conventional three-electrode system. The auxiliary electrode was a platinum wire and the potential values were referred to the Ag pseudo-reference electrode. The CV results (as shown in figure below) demonstrated that the composite hydrogels exhibited both peak of oxidation and reduction. However, if you don't mind, we need to keep this data for our on-going project. Therefore, we prefer to show this data for our next publication.



ARTICLE

Self-Healing Composite Hydrogel with Antibacterial and Reversible Restorability Conductive Properties

Mimpin Ginting^{a†*}, Subur P. Pasaribu^{b†}, Indra Masmur^a, Jamaran Kaban^a, and Hestina^c

Received 00th January 20xx,
Accepted 00th January 20xx

DOI: 10.1039/x0xx00000x

Self-healable PAA/PPy-Fe composite hydrogels have been simply synthesized in one step preparation and utilized for antibacterial and electrical conductivity application. The network of hydrogel composed of polyacrylic acid (PAA) and Fe³⁺ ions with the interlace of the second polymeric chain of polypyrrole (PPy). In this study, ammonium persulfate (APS) was utilized to initiate the polymerization of both acrylic acid and pyrrole. Such hydrogels exhibited good mechanical properties and remarkable self-healing efficiency as well. The self-healing ability of the hydrogels was facilitated by ionic interaction between carboxylic anion groups (COO⁻) from polyacrylic acid (PAA) and Fe³⁺ ions. Moreover, the antibacterial activity of the composite hydrogels was examined on *Escherichia coli* via disk diffusion method and the zone of inhibition was obtained in the range of 1.26 – 1.56 cm after incubated for 12 h. In addition, the demonstration of the PAA/PPy-Fe composite hydrogels in electrical conductivity application was performed in which the composite hydrogel was set up in an electrical circuit consisted of LED and powered by 3 V batteries. The results showed that the electricity lighted-up the LED through the PAA/PPy-Fe composite hydrogels and possessed reversible restorability indicated by the healed hydrogel consistently lighting-up the LED in the electrical circuit.

Introduction

Self-healing hydrogels are 3D cross-linked hydrophilic polymer networks and able to repair or restore to the original functionalities automatically after being damaged without any external stimuli. Hydrogels provide superior properties such as retain considerable amounts of water, biocompatibility, biodegradable, and elasticity¹⁻³. Owing to such properties, hydrogels have attracted considerable attention and widely used in drug delivery, wound healing, bio-inspired materials, biosensors and many other applications⁴⁻⁷. On the other hand, there are remaining challenges; in particular, the lifespan and durability of hydrogels such as poor mechanical properties⁸. Acrylic acid is the monomer of poly(acrylic acid) (PAA) which contain unsaturated carboxylic acid groups and tend to be hydrophilic, exhibit good absorption ability and responsive to pH. Due to the ionic character of the carboxylic groups (-COOH), PAA can be cross-linked with multivalent ions. For instance, Wei et al. (2013) synthesized a self-healing hydrogel induced by the migration of ferric ions (Fe³⁺) which was applied as a protective coating where the hydrogel can protect the glass against mechanical damage². Meanwhile, the self-healing hydrogel of

amorphous calcium carbonate (CaCO₃)-polyacrylic acid has been fabricated to substitute the conventional plastics⁷. Recently, Pan et al. (2019) reported the preparation of triple-physical crosslinking (coordination, hydrogen and electrostatic interactions) self-healing hydrogel by utilizing PAA, Aluminium ions (Al³⁺), and carboxymethyl chitosan nanoparticles which possesses antibacterial properties⁹. However, the reported self-healing hydrogels do not possess conductive properties which might be interesting. Furthermore, hydrogels are usually vulnerable to microorganisms during applications, leading possible infection which is a serious issue. To address this problem, various hydrogels with antimicrobial properties involved multi-steps syntheses were reported^{10, 11}.

For the last few decades, conductive polymers, such as polyaniline (PANI), polythiophene (PT), polypyrrole (PPy), and poly(3,4-ethylene dioxythiophene) (PEDOT) have drawn researchers' attention due to its electrical properties which are originated from the conjugated π -electron backbone (double bond). The delocalization of electrons is contained in π -bond in which the electrons are free to move over more than two nuclei¹²⁻¹⁴. The conducting polymers were widely used in various application such as biosensors¹⁵, artificial muscles¹⁶, drug delivery¹⁷, and supercapacitors¹⁸. The resultant conducting polymers in most cases are rigid and brittle as a consequence of the delocalized π -electron backbone.

Driven by the challenges of enabling the conductive properties of self-healing hydrogels and to solve the rigidity issue of conducting polymers, herein we reported a simple approach to fabricate PAA/PPy-Fe composite hydrogels with self-healing, antibacterial, and conductive properties. The PAA/PPy-Fe composite hydrogels were synthesized via free-radical

^a Department of Chemistry, Faculty of Mathematics and Natural Sciences, Universitas Sumatera Utara, Medan-20155, Indonesia.

^b Department of Chemistry, Faculty of Mathematics and Natural Sciences, Mulawarman University, Samarinda-75123, Indonesia

^c Department of Chemistry, Universitas Sari Mutiara Indonesia, Medan-20123, Indonesia.

† Ginting, M. and Pasaribu S.P. contributed equally to this work.

Electronic Supplementary Information (ESI) available: [details of any supplementary information available should be included here]. See DOI: 10.1039/x0xx00000x

polymerization. To the best of our knowledge, no study has been reported to synthesize PAA/PPy-Fe composite hydrogels in one-step preparation.

Materials and methods

Materials

Acrylic acid (CH₂CHCOOH, 99.1%, Echo Chemical), iron (III) chloride anhydrous (FeCl₃, 98%, Sigma-Aldrich), pyrrole (C₄H₅N, 99%, Acros Organics), ammonium persulfate ((NH₄)₂S₂O₈, 98%, Sigma-Aldrich), and HCl (37%, Sigma-Aldrich) were analytical grade and used as received without further treatment.

Preparation of PAA/PPy-Fe hydrogels

AA solution with the concentration of 30 w/v% was prepared by dissolving in deionized water, followed by FeCl₃ addition of 0.5 mol% of AA with continuous stirring. Afterwards, pyrrole with concentration varied from 5 – 20 mM were mixed in the solution of AA-FeCl₃. The mixture solution was degassed by using N₂ for 30 minutes. Then, the solution was transferred to a petri dish with an internal diameter of 5 cm and polymerization was performed by adding APS with an amount of 0.15 mol% of AA and conducted at 37°C for 24 h. On the other hand, the hydrogels without PPy was also synthesized as the control group. Additionally, for the study of Fe³⁺ concentration on hydrogel properties, the concentrations of Fe³⁺ were varied from 0.1 to 0.3, 0.5, 0.7 and 1 mol% of AA while the concentration of pyrrole was fixed at 15 mM. Furthermore, the as-prepared hydrogels were washed by DI water and alcohol for several times to remove unreacted monomers and used for further characterization. For the nomenclature, the obtained hydrogel was named as PAA/PPy_n-Fe where n refers to the concentration of pyrrole (e.g. PAA/PPy₁₀-Fe).

FTIR analysis

Samples were analyzed as a powder mixed with KBr powder by Fourier transform infrared method. Spectra were collected in the wavenumber of 4000-400 cm⁻¹, a scan number of 64 and a resolution of 4 cm⁻¹ using a Bio-Rad Model FTS-3500GX spectrometer.

Equilibrium Degree of swelling (DS) and gel fraction (GF)

Equilibrium swelling degree of the as-prepared hydrogels was determined by gravimetric method. Firstly, the hydrogel samples were immersed in DI water at 37°C for 48 hours. Subsequently, the swollen hydrogels were wiped gently in order to remove the water excess from the surface and weigh as W_s using an analytical balance. In addition, the effect of pH (1-7) on swelling degree of PAA/PPy-Fe composite hydrogel was also studied. The pH of the swelling solution was adjusted by adding HCl. The equilibrium degree of swelling was calculated by the following equation:

$$DS = \frac{W_s - W_d}{W_d} \times 100\%$$

From the swelling experiment, the swollen hydrogels were then dried in an oven at 70°C until a constant weight was obtained and recorded as W_d', the gel fraction was calculated by the following equation:

$$GF = \frac{W_d'}{W_d} \times 100\%$$

Both swelling and gel fraction experiments were repeated three times and expressed the results as mean ± standard deviation (SD).

Mechanical Properties and self-healing efficiency

The composite hydrogels samples were cut into two pieces and allowing the self-healing at 37°C for 12 h without any external stimulation. Afterwards, the healed hydrogels were subjected to tensile tests (Testometric M500-25AT) with a 100 N load cell and a crosshead speed of 50 mm/min at room temperature. Finally, the self-healing efficiency of hydrogels is calculated by the following equation:

$$\eta = \frac{\sigma'}{\sigma} \times 100\%$$

Where σ and σ' represent tensile stress of pristine and healed hydrogels, respectively. The tests were conducted in triplicate for each specimen and expressed the results as mean ± standard deviation (SD).

SEM and EDX analyses

The surface morphology of PAA/PPy-Fe composite hydrogels was investigated with a JEOL (JSM-6500F, Tokyo, Japan) FE-SEM at an accelerating voltage of 10 kV. Previous to the scanning process, the samples were coated by a thin layer of platinum through the sputtering process. At the same time, energy dispersive X-ray (EDX) spectroscopy was performed to identify the elemental composition of hydrogels.

Antibacterial activity

Antibacterial activity of hydrogels was investigated via a disk diffusion method using *Escherichia coli* as gram-negative bacteria with a final OD₆₀₀ = 0.05 which were cultivated on overnight Luria-Bertani (LB) culture plate at 37°C. The samples were adhered on the top of bacteria-suspended LB plate and kept with face-down position at 37°C. Then, the antibacterial activity of samples was determined by measuring the inhibition zone of the samples after incubated for 8 and 12 h.

Electrical properties

The electrical properties of PAA/PPy-Fe hydrogels were characterized by using a conventional four-point probe technique to measured sheet resistance, using a set of Napson RT-7 and RG-7. PAA/PPy-Fe films were deposited on a glass slide and the thickness of the films was analyzed by surface profiler (Veeco Dektak 150 Stylus Profilometer). However, prior to the measurement, the water content in the hydrogels was maintained at 50% in order to eliminate the possibility of water

in affecting the conductivity of hydrogels. The measurements were conducted in triplicate and expressed the results as mean \pm standard deviation (SD). Moreover, the resistivity was calculated from resistance and film thickness, while conductivity (σ) of the sample was calculated using the following equation:

$$R = \frac{1}{R \times t}$$

Where R denotes as sheet resistance and t represent the thickness of the film. Moreover, the resistant changes as a function of the strain of PAA/PPy-Fe composite hydrogels were measured using an oscilloscope (Tektronix DPO2012B).

Electrical conductivity application

The electrical conductivity application of PAA/PPy-Fe hydrogels was evaluated through a simple electrical circuit consisting of a light-emitting diode (LED) which was powered by 3 V batteries and connected with PAA/PPy-Fe hydrogels as illustrated in Fig. 1. To show the reversible restorability of PAA/PPy-Fe hydrogels, the hydrogel was cut-off and allowed to heal. Finally, the healed hydrogel was reconnected into the electrical circuit. The demonstration of PAA/PPy-Fe in conducting electricity in the circuit as indicated by the light on/off of LED.

(Figure 1)

Results and discussion

Preparation of PAA/PPy-Fe hydrogels

In this study, PAA/PPy-Fe composite hydrogels with fixed Fe content (0.5 mol% of AA) and variation of pyrrole concentration (0 – 20 mM) were fabricated. On the other hand, the hydrogels by varying Fe concentration (0.1 – 1 mol% of AA) and a fixed amount of pyrrole (15 mM) were synthesized. Firstly, the polymerization of AA and pyrrole was initiated by APS through free-radical polymerization (FRP). Prior to the polymerization, the mixture solution was degassed by using N₂ in order to remove O₂ contained in the solution, which can scavenge the radical during polymerization¹⁹. Further, the composite hydrogels were obtained by cross-linking (ionic interaction) between COO⁻ from PAA and Fe³⁺ from FeCl₃. The cross-linked hydrogels are able to heal autonomously after being damaged as shown in Fig. 2 which is ascribed to that ionic interaction. Moreover, the healed hydrogel could withstand stretching (Fig. 2b(iii)). Additionally, the self-healing processes observed by SEM displayed that both of the interfaces of the cut-off hydrogel adhered to each other. Such autonomous self-healing occurred in 3 h at 37°C and showed no significant difference after healed for 12 h as shown in Fig. 1S. Moreover, the hydrogels also possessed antimicrobial properties and conductive properties due to polypyrrole in the hydrogels.

(Figure 2)

Chemical Functionalities by FTIR analysis

The spectra of chemical functionalities of hydrogels are presented in Fig. 3. The peak at wavenumber 1650 cm⁻¹ appeared in the spectra of acrylic acid corresponds to the C=C stretching vibration. In the spectra of hydrogels, the peak of C=C decreased significantly compared to the spectra of AA, which assigned to the polymerization of AA. The shifting peak from 1720 cm⁻¹ (C=O) in AA spectrum to 1711 cm⁻¹ in hydrogels spectra was assigned to the ionic interaction between carboxylic groups (COO⁻) from PAA and Fe³⁺. As for the spectra of PAA/PPy-Fe composite hydrogels, the peaks at 1600 and 730 cm⁻¹ were attributed to the bending vibrations of N-H and C-H of N-substituted of PPy, respectively. Furthermore, the stretching vibration of N-H from PPy is found in the range of 3400-3500 cm⁻¹ which is overlapped with OH stretching vibration. However, by varying concentration of pyrrole, the spectra of PAA/PPy-Fe hydrogels indicated insignificant alteration of the functional groups.

(Figure 3)

Equilibrium degree of swelling and gel fraction

The equilibrium degree of swelling and gel fraction of PAA/PPy-Fe hydrogels were shown in Fig. 4a. The results of swelling degree were 146.2, 118.5, 112.5, 71.9, and 44.8 % for PAA-Fe, PAA/PPy₅-Fe, PAA/PPy₁₀-Fe, PAA/PPy₁₅-Fe, and PAA/PPy₂₀-Fe, respectively. The gel fraction decreased gradually from 88.7 % to 67.1 % with increasing concentration of pyrrole from 0 mM to 20 mM. The degrading values of gel fraction with increasing pyrrole concentration were ascribed to that pyrrole monomers react with FeCl₃ through oxidative polymerization²⁰ and resulted in less ionic interaction between COO⁻ from AA and Fe³⁺ from FeCl₃. Likewise, in the variation of Fe concentration, the swelling ratio showed a declining value from 169.9 to 40.1 % as increase Fe concentration. On the contrary, the gel fraction of the prepared hydrogels increased from 27.9 to 98.8 % with increasing Fe concentration. In this regards, such low gel fraction hydrogels contained less cross-linking junctions and less dense network, thus are able to expand more and absorb more water. Therefore, low gel fraction resulted in a high degree of swelling of the hydrogels. On the other hand, the swelling behaviour of PAA/PPy-Fe composite hydrogels was investigated in the pH range of 1-7 and represented in Fig. 4b. In this experiment, PAA/PPy₁₀-Fe was used as a representative to study the swelling behavior at different pH. Moreover, the ability of the hydrogel in retaining water increased gradually with increasing pH (1-7) of the swelling solution, which is ranged from 40.1 % to 112.5 %. The reason of such increasing trend at higher pH is due to the deprotonation of COOH groups in PAA (pKa= 4.2) which cause the electrostatic repulsion and enlarge the networks in the hydrogel^{21, 22}.

(Figure 4)

Mechanical Properties and self-healing efficiency

The tensile stress of PAA-Fe reached 0.83 MPa and with the addition of pyrrole with the concentration of 5, 10, 15, and 20 mM, the tensile stress was found to be 0.77, 0.64, 0.52, and 0.39 MPa, respectively. These results proved that the increase in

pyrrole concentration could weaken the tensile stress of PAA/PPy-Fe composite hydrogels as can be seen in Fig. 5a. The result of gel fraction echoed such trend of tensile stress in which with the decrease of the cross-link density, the tensile stress will decrease²³. Despite that, the PAA/PPy-Fe composite hydrogels show improvement in tensile strain from 180 % to 448% with increasing pyrrole concentration from 5 to 20 mM. Subsequently, the self-healing efficiency of PAA/PPy-Fe composite hydrogels was evaluated by comparing the tensile stress of pristine and healed hydrogels. Herein, the fractured hydrogels were healed at 37°C for 12 h prior to the tensile tests. The tensile test results of healed hydrogels (σ') displayed a decreasing trend from 0.57 MPa to 0.17 MPa with increasing pyrrole concentration from 5 mM to 20 mM. Hence, the self-healing efficiency (η) was calculated to be 74.1 %, 61.6 %, 50.8 %, and 42.69 % for PAA/PPy₅-Fe, PAA/PPy₁₀-Fe, PAA/PPy₁₅-Fe, and PAA/PPy₂₀-Fe, respectively (Fig. 5c). On the other hand, by increasing Fe concentration (0.1 – 1 mol% of AA), tougher hydrogels were produced in which the tensile stress increased from 0.31 – 0.74 MPa. As indicated by the result of tensile strain, the resulted hydrogels got more rigid and brittle with increasing Fe concentration. However, in agreement with the result of tensile stress, the self-healing efficiency of hydrogels exhibited a better result with increasing Fe concentration which raised from 33.37% to 70.58% (Fig. 5d). The decreasing in self-healing efficiency (η) might be correlated to the gel fraction of hydrogels, in which there might be less ionic interaction (-COO-Fe³⁺) between the interface of two separated halves at lower gel fraction, therefore decrease the self-healing efficiency (η). Likewise, the results of both self-healing efficiency and gel fraction indicated a similar trend.

(Figure 5)

Surface morphology of hydrogels

The surface morphology of PAA/PPy-Fe composite hydrogels was observed using SEM and the images are depicted in Fig. 6(i-viii). As can be seen in the figure, all hydrogels exhibited a relative smooth surface. However, as pyrrole concentration increases, there are more particles can be observed on the surface of hydrogels which probably arises from polypyrrole. On the other hand, EDX analysis was performed to determine the elemental composition of PAA/PPy-Fe composite hydrogels. The EDX spectra of the hydrogels are presented in Fig. 6(ix-xii) and their elemental composition are summarized in Table 1. The results of EDX analysis revealed the presence of polypyrrole in the hydrogels indicated by N element and the atomic % of N increased with increasing of the pyrrole concentration.

(Figure 6)

(Table 1)

Antibacterial activity

The antibacterial activity of PAA/PPy-Fe composite hydrogels was investigated toward *Escherichia coli* with a final OD₆₀₀ value = 0.05. In this experiment, 10 μ L of H₂O₂ on filter paper was used as the control group and all of the samples were cut with a size

of 4 mm (Fig. 7a and b). The results revealed that the average diameter of inhibition zone incubated for 8 h increased slightly from 1.72 cm to 1.78, 1.86, and 1.87 cm for PAA/PPy₅-Fe, PAA/PPy₁₀-Fe, PAA/PPy₁₅-Fe, and PAA/PPy₂₀-Fe hydrogels, respectively (Fig. 7c). However, at longer incubation time of 12 h, the bactericidal abilities of composite hydrogels decreased and were found in the range of 1.26 – 1.56 cm. In this regard, both ferric ions (Fe³⁺) and polypyrrole played an important role for the antibacterial properties in which the antibacterial mechanism of Fe³⁺ is the adsorption of Fe³⁺ on the bacteria and subsequently reduced to ferrous ions (Fe²⁺)^{24, 25}. Meanwhile, the positively charged polypyrrole seems to be responsible for the antibacterial activity by interacting with the bacterial cell wall and resulted in the death of bacteria^{26, 27}.

(Figure 7)

Electrical Properties

The electrical properties (resistivity and conductivity) of PAA/PPy-Fe composite hydrogels were measured by the four-point probe method. Fig. 8a revealed that the resistivity of hydrogels decreased from 4.84 k Ω to 1.09 k Ω with increasing pyrrole concentration from 5 – 20 mM and at the same time, the electroconductivity increased from 0.21 S m⁻¹ to 0.92 S m⁻¹. The increase in pyrrole concentration indicated an increase in conductivity as well and showed a good agreement with the results reported by Gan, et. al. (2018) and Ren, et. al. (2019)^{28, 29}. Likewise, at higher cross-linking density, the rigid network was obtained and lead to hindrance for ions migration in the hydrogel networks therefore increase the resistance³⁰. In addition, the resistance changes of composite hydrogel under strain were investigated and PAA/PPy₂₀-Fe hydrogel was used because it possesses the highest conductivity to compare to the other. Briefly, the resistance of PAA/PPy₂₀-Fe hydrogel increased with the increasing strain which was found to be 380 % when the gel was stretched to 100 % as can be seen in Fig. 8b. In this case, Fe³⁺ serves as dopant (oxidant) and Cl⁻ as a counter ion to be incorporated into the *p*-doped polypyrrole ring, in which the conductive properties arise from the oxidized form of polypyrrole-Cl³¹.

(Figure 8)

Electrical conductivity applications

The application of PAA/PPy-Fe composite hydrogels was evaluated by constructing a simple electrical circuit consisted of PAA/PPy₁₅-Fe connected with a light-emitting diode (LED) which was powered by 3 V batteries. PAA/PPy₁₅-Fe hydrogel was used by considering its self-healing efficiency and conductivity. After the electric was given, LED in the circuit was lighted-up which indicated the ability of PAA/PPy₁₅-Fe hydrogels to conduct electricity from the battery to LED as can be seen in Fig. 9a and b (stretched). In order to evaluate the reversible restorability, the hydrogel was cut into two-separated halves and the circuit was disconnected indicated by light-off as depicted in Fig. 9c. Then, the two broken pieces were allowed to heal at 70°C for 2 h and reconstructed into the circuit. The result for after healed hydrogel proved that the LED can be lighted up again as shown

in Fig. 9d and e (stretched). Nevertheless, as a result of resistance changes of PAA/PPy-Fe hydrogels under strain, the light intensity of LEDs was decreased (dim) when connected to both stretched pristine and healed hydrogels which can be seen visually in Fig. 9b and e.

(Figure 9)

Conclusion

In conclusion, self-healable PAA/PPy-Fe composite hydrogels with antimicrobial and conductive properties have been fabricated via free-radical polymerization in single-step preparation. The PAA/PPy-Fe composite hydrogels possess satisfying self-healing efficiency, bactericidal abilities and high in conductivity. The formation of PAA/PPy-Fe composite hydrogels is confirmed by the analyses of FTIR, SEM, and EDX. Furthermore, gel fraction (cross-linking density) of PAA/PPy-Fe composite hydrogels also plays a crucial role in the swelling, mechanical, and electrical properties of the resultant hydrogels. In addition, all the PAA/PPy-Fe composite hydrogels have been tested for their antibacterial activity on *Escherichia coli* and the result demonstrates that with higher pyrrole concentration, PAA/PPy-Fe composite hydrogels possess higher bactericidal effects. On the other hand, due to the conductive properties of PAA/PPy-Fe hydrogels, the hydrogel conducts electricity by lighting up the LED in an electrical circuit. Interestingly, the hydrogel demonstrates reversible restorability which is indicated by the healed hydrogel consistently conducts the electricity and lights up the LED.

Conflicts of interest

There are no conflicts to declare.

Acknowledgements

The authors would thank Universitas Sumatera Utara (USU) for the facilities to conduct the research.

Notes and references

1. Y. H. Tsou, J. Khoneisser, P. C. Huang and X. Xu, *Bioact Mater*, 2016, **1**, 39-55.
2. Z. Wei, J. He, T. Liang, H. Oh, J. Athas, Z. Tong, C. Wang and Z. Nie, *Polymer Chemistry*, 2013, **4**, 4601.
3. W. Wang, R. Narain and H. Zeng, *Front Chem*, 2018, **6**, 497.
4. H. R. Culver, J. R. Clegg and N. A. Peppas, *Acc Chem Res*, 2017, **50**, 170-178.
5. A. S. Hoffman, *Advanced Drug Delivery Reviews*, 2012, **64**, 18-23.
6. N. A. Peppas, J. Z. Hilt, A. Khademhosseini and R. Langer, *Advanced Materials*, 2006, **18**, 1345-1360.
7. S. Sun, L. B. Mao, Z. Lei, S. H. Yu and H. Colfen, *Angew Chem Int Ed Engl*, 2016, **55**, 11765-11769.
8. M. Zhong, Y. T. Liu, X. Y. Liu, F. K. Shi, L. Q. Zhang, M. F. Zhu and X. M. Xie, *Soft Matter*, 2016, **12**, 5420-5428.
9. J. Pan, Y. Jin, S. Lai, L. Shi, W. Fan and Y. Shen, *Chemical Engineering Journal*, 2019, **370**, 1228-1238.
10. H. Wang, G. Zha, H. Du, L. Gao, X. Li, Z. Shen and W. Zhu, *Polym. Chem.*, 2014, **5**, 6489-6494.
11. D. Gan, T. Xu, W. Xing, X. Ge, L. Fang, K. Wang, F. Ren and X. Lu, *Advanced Functional Materials*, 2019, **29**.
12. J. H. Min, M. Patel and W. G. Koh, *Polymers (Basel)*, 2018, **10**.
13. G. Kaur, R. Adhikari, P. Cass, M. Bown and P. Gunatillake, *RSC Advances*, 2015, **5**, 37553-37567.
14. D. L. Wise, G. E. Wnek, D. J. Trantolo, T. M. Cooper, J. D. Gresser and D. Marcel, *Electrical and Optical Polymer Systems: Fundamentals, Methods, and Application*, Marcel Dekker, New York, 1998.
15. R. K. Pal, S. Pradhan, L. Narayanan and V. K. Yadavalli, *Sensors and Actuators B: Chemical*, 2018, **259**, 498-504.
16. A. Simaite, F. Mesnilgrente, B. Tondu, P. Souères and C. Bergaud, *Sensors and Actuators B: Chemical*, 2016, **229**, 425-433.
17. D. Uppalapati, B. J. Boyd, S. Garg, J. Travas-Sejdic and D. Svirskis, *Biomaterials*, 2016, **111**, 149-162.
18. V. Khomenko, E. Frackowiak, V. Barsukov and F. Beguin, *New Carbon Based Materials for Electrochemical Energy Storage Systems*, 2006, 41-50.
19. V. A. Bhanu and K. Kishore, *Chemical Reviews*, 1991, **91**, 99-117.
20. Y. Lu, W. He, T. Cao, H. Guo, Y. Zhang, Q. Li, Z. Shao, Y. Cui and X. Zhang, *Sci Rep*, 2014, **4**, 5792.
21. E. O. Akala, P. Kopeckova and J. Kopecek, *Biomaterials*, 1998, **19**, 1037-1047.
22. J. E. Elliott, M. Macdonald, J. Nie and C. N. Bowman, *Polymer*, 2004, **45**, 1503-1510.
23. B. Depalle, Z. Qin, S. J. Shefelbine and M. J. Buehler, *J Mech Behav Biomed Mater*, 2015, **52**, 1-13.
24. R. Tian, X. Qiu, P. Yuan, K. Lei, L. Wang, Y. Bai, S. Liu and X. Chen, *ACS Appl Mater Interfaces*, 2018, **10**, 17018-17027.
25. H. Q. Sun, X. M. Lu and P. J. Gao, *Brazilian Journal of Microbiology*, 2011, **42**, 410-414.
26. A. Varesano, C. Vineis, A. Aluigi, F. Rombaldoni, C. Tonetti and G. Mazzuchetti, *Fibers and Polymers*, 2013, **14**, 36-42.
27. W. Zhou, L. Lu, D. Chen, Z. Wang, J. Zhai, R. Wang, G. Tan, J. Mao, P. Yu and C. Ning, *Journal of Materials Chemistry B*, 2018, **6**, 3128-3135.
28. D. Gan, L. Han, M. Wang, W. Xing, T. Xu, H. Zhang, K. Wang, L. Fang and X. Lu, *ACS Appl Mater Interfaces*, 2018, **10**, 36218-36228.
29. K. Ren, Y. Cheng, C. Huang, R. Chen, Z. Wang and J. Wei, *J Mater Chem B*, 2019, **7**, 5704-5712.
30. W. K. Shin, J. Cho, A. G. Kannan, Y. S. Lee and D. W. Kim, *Sci Rep*, 2016, **6**, 26332.
31. R. Buitrago-Sierra, M. J. García-Fernández, M. M. Pastor-Blas and A. Sepúlveda-Escribano, *Green Chemistry*, 2013, **15**.

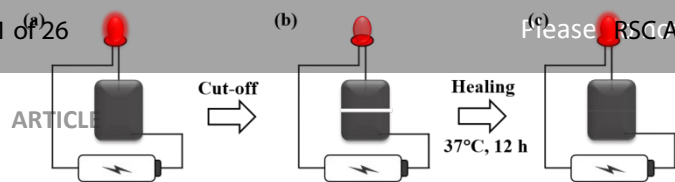


Figure 1. Schematic illustration of an electrical circuit consisted of LED, powered by the battery and connected through (a) initial; (b) cut-off; and (c) healed PAA/PPy-Fe hydrogel.

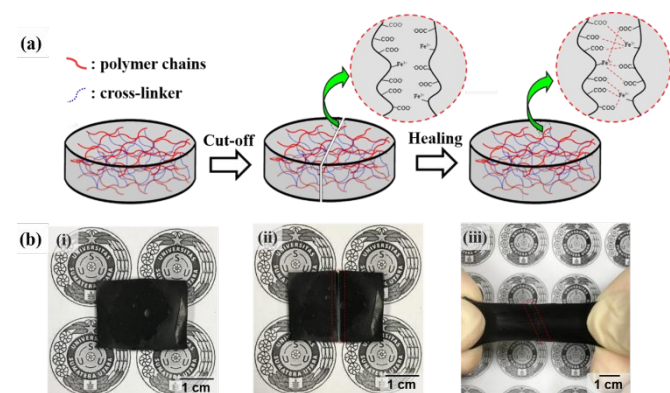


Figure 2. (a) Illustration of self-healing processes of PAA/PPy-Fe hydrogels via ionic interaction and (b) photographs of PAA/PPy-Fe hydrogels in the condition of: (i) initial; (ii) cut-off; and (iii) healed hydrogel under stretching.

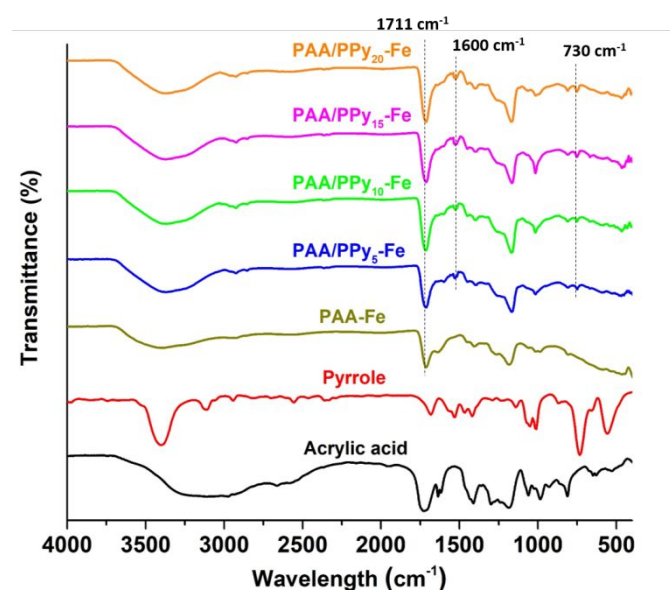


Figure 3. FTIR spectra of acrylic acid, pyrrole and hydrogels with a variation of pyrrole concentration.

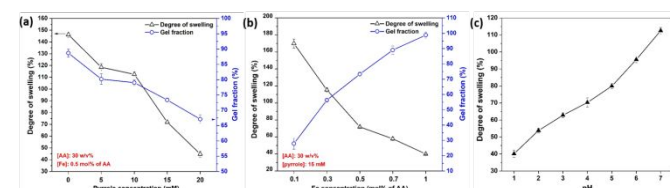


Figure 4. Degree of swelling and gel fraction of hydrogels with (a) variation of pyrrole concentration; (b) variation of Fe concentration; and (c) the effect of pH on the swelling degree of PAA/PPy-Fe hydrogel.

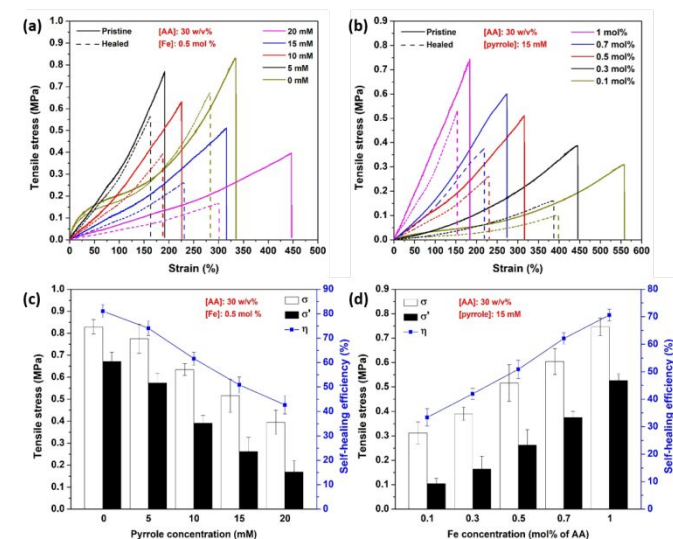


Figure 5. Mechanical properties of tensile stress-strain curves of hydrogels with (a) variation of pyrrole concentration; and (b) variation of Fe concentration. Tensile stress-self-healing efficiency graphs of hydrogels with (c) variation of pyrrole concentration; and (d) variation of Fe concentration.

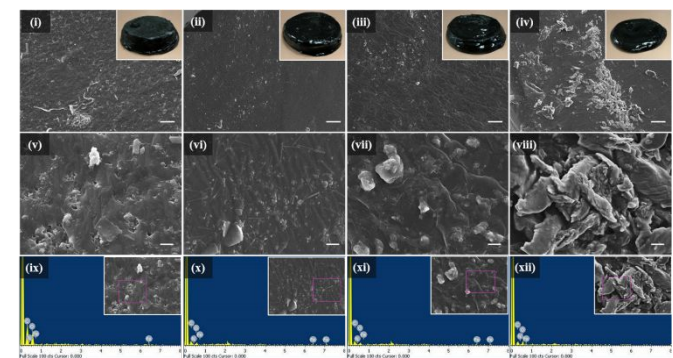


Figure 6. SEM images of freeze-dried hydrogels: (i) PAA/PPy₅-Fe; (ii) PAA/PPy₁₀-Fe; (iii) PAA/PPy₁₅-Fe; and PAA/PPy₂₀-Fe hydrogels at magnification of x500, (v-viii) at x5000 and the EDX spectrum of hydrogels (ix – xii). Scale bars are (i-iv) 20 μm and (v-viii) 2 μm.

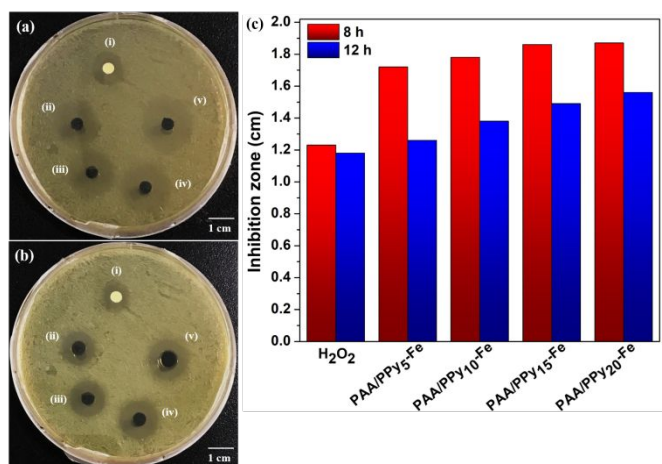
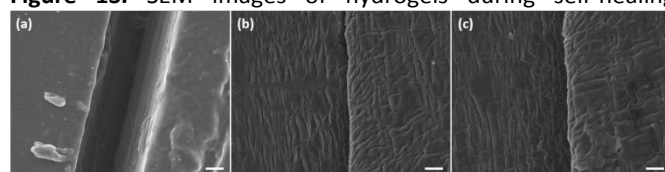


Figure 7. Antibacterial activity of hydrogels: (i) H₂O₂; (ii) PAA/PPy₅-Fe; (iii) PAA/PPy₁₀-Fe; (iv) PAA/PPy₁₅-Fe; and (v) PAA/PPy₂₀-Fe on *E.coli* bacteria incubated at 37°C for: (a) 8 h; (b) 12 h and (c) zone of inhibition of PAA/PPy-Fe hydrogels with different composition.

Table 1. The elements composition by EDX analysis of PAA/PPy-Fe composite hydrogels.

Hydrogels	Elements (atomic %)				Total (%)
	C	N	O	Fe	
PAA/PPy ₅ -Fe	55.86	1.01	41.98	1.15	100
PAA/PPy ₁₀ -Fe	47.09	9.32	40.77	2.82	
PAA/PPy ₁₅ -Fe	40.92	19.31	39.18	0.58	
PAA/PPy ₂₀ -Fe	40.49	20.67	38.01	0.83	

Figure 1S. SEM images of hydrogels during self-healing



processes (a) cut-off; healed at 37°C for (b) 3 h; and (c) 12 h at magnification of x1000 (scale bar 10µm).

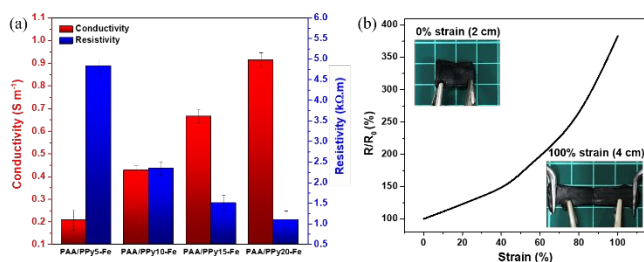


Figure 8. (a) the electroconductivity and resistivity of PAA/PPy-Fe hydrogels with various concentration of pyrrole and (b) resistance ratio-strain curve of PAA/PPy₂₀-Fe hydrogel (the inserted photos are the strain at 0 and 100%).

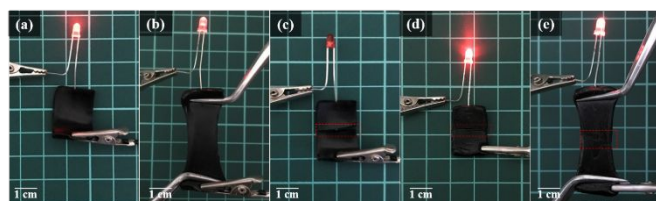


Figure 9. Photographs of PAA/PPy-Fe hydrogel conducting electricity in an electrical circuit, (a) original; (b) stretched; (c) cut-off; (d) healed; and (e) healed and stretched hydrogel.

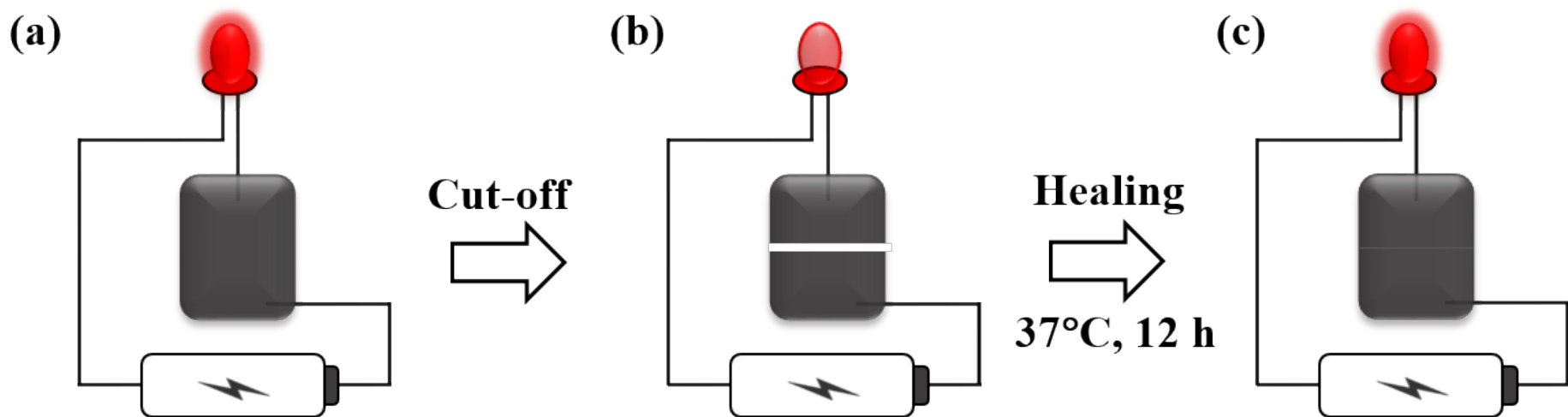


Figure 1. Schematic illustration of an electrical circuit consisted of LED, powered by the battery and connected through (a) initial; (b) cut-off; and (c) healed PAA/PPy-Fe hydrogel.

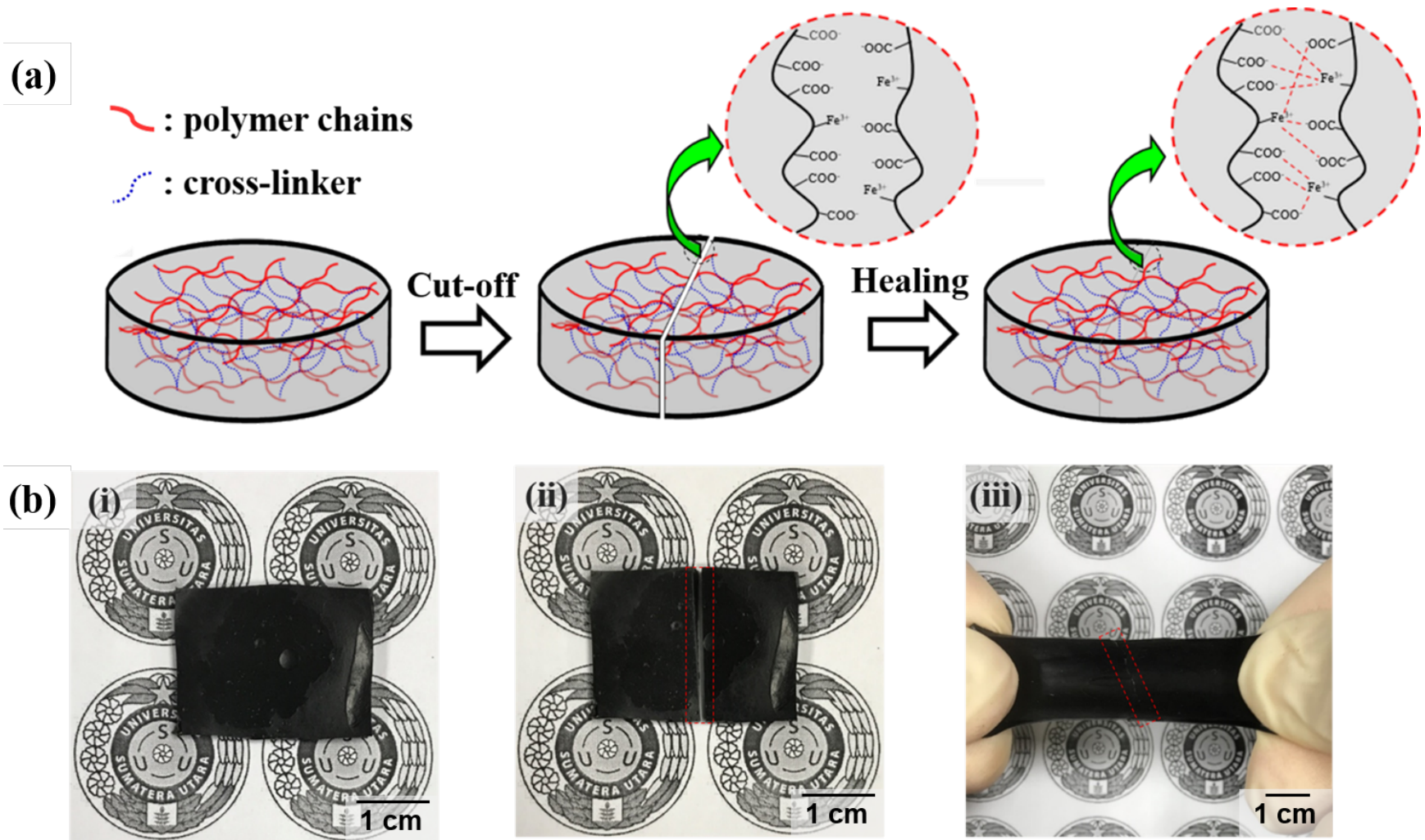


Figure 2 (a) Illustration of self-healing processes of PAA/PPy-Fe hydrogels via ionic interaction and (b) photographs of PAA/PPy-Fe hydrogels in the conditions of: (i) initial; (ii) cut-off; and (iii) healed hydrogel under stretching.

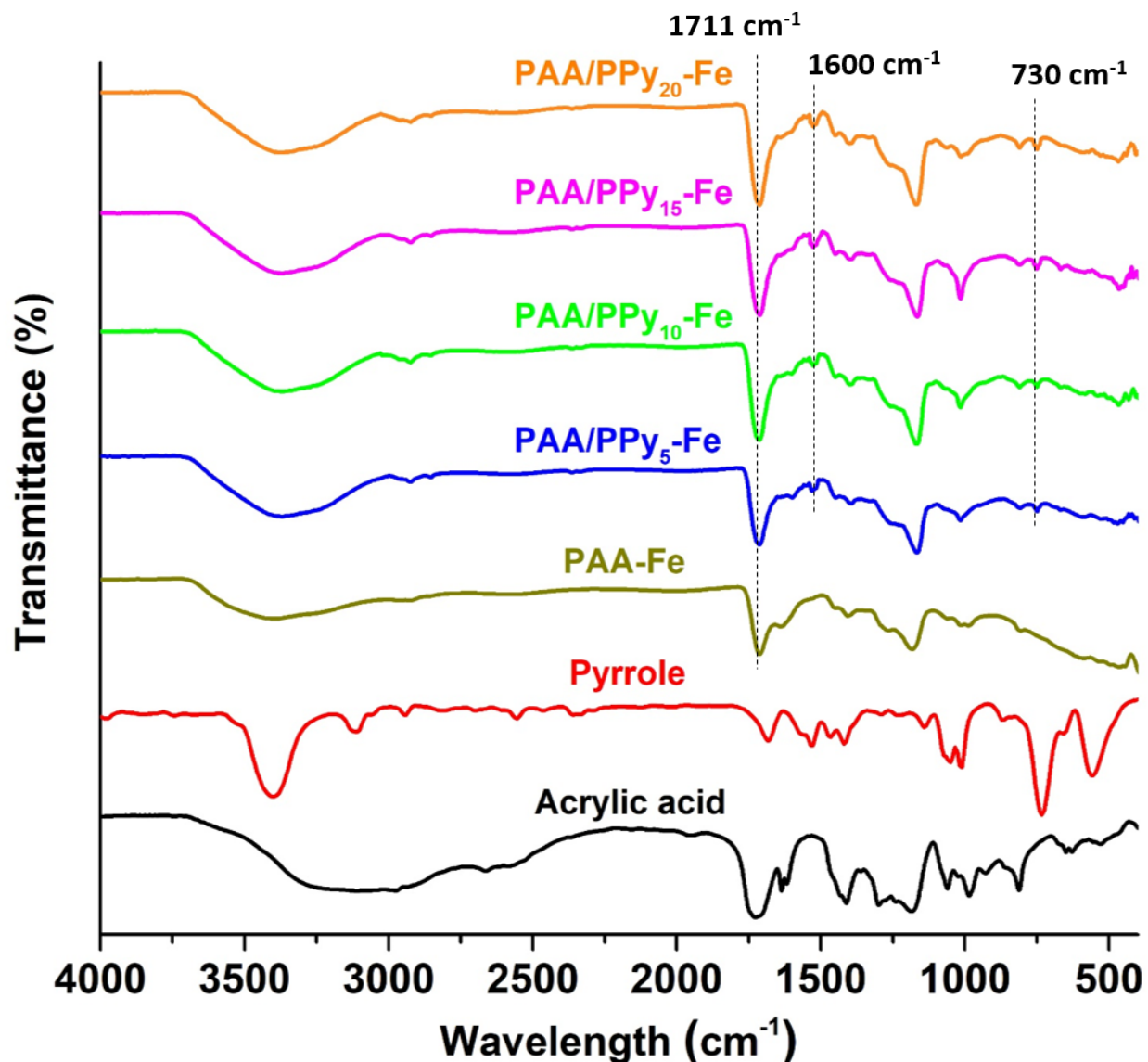


Figure 3 FTIR spectra of acrylic acid, pyrrole and hydrogels with a variation of pyrrole concentration.

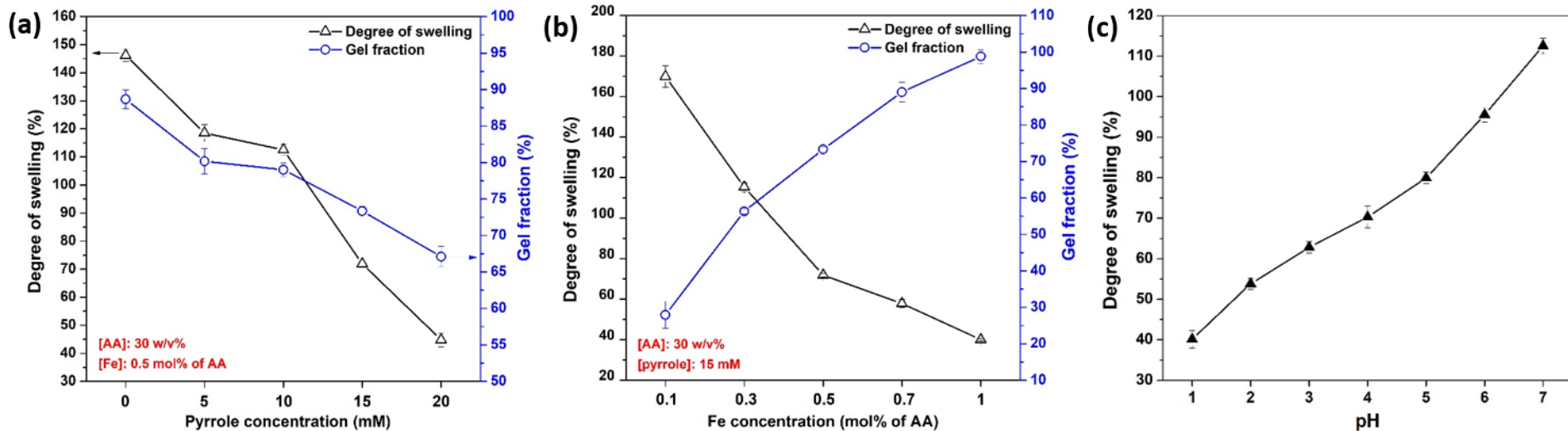


Figure 4 Degree of swelling and gel fraction of hydrogels with (a) variation of pyrrole concentration; (b) variation of Fe concentration; and (c) effect of pH on the swelling degree of PAA/PPy-Fe composite hydrogel

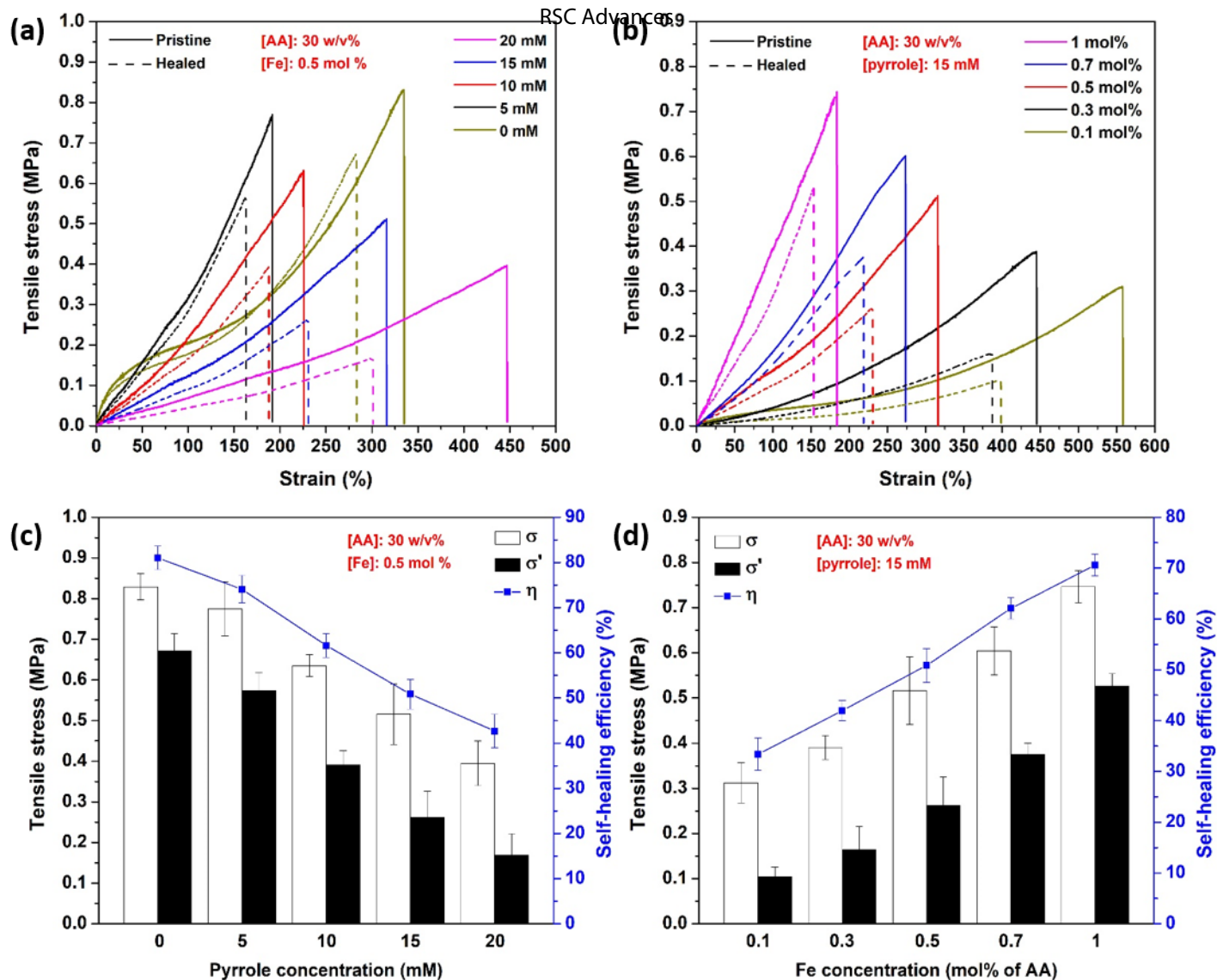


Figure 5 Mechanical properties of tensile stress-strain curves of hydrogels with (a) variation of pyrrole concentration; and (b) variation of Fe concentration. Tensile stress-self-healing efficiency graphs of hydrogels with (c) variation of pyrrole concentration; and (d) variation of Fe concentration

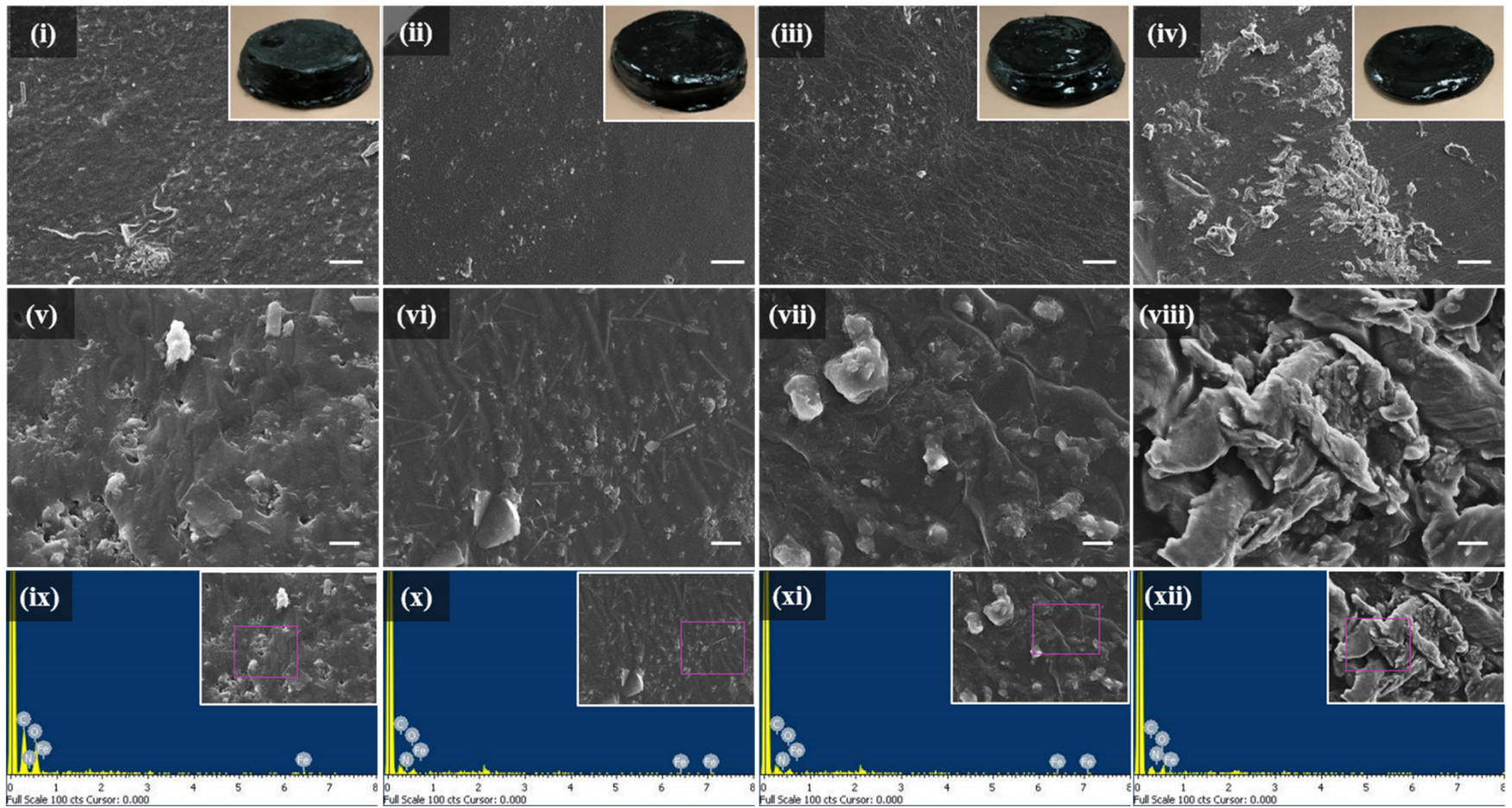


Figure 6 SEM images of freeze-dried hydrogels: (i) PAA/PPy₅-Fe; (ii) PAA/PPy₁₀-Fe; (iii) PAA/PPy₁₅-Fe; and PAA/PPy₂₀-Fe hydrogels at magnification of x500, (v–viii) at x5000 and the EDX spectrum of hydrogels (ix – xii). Scale bars are (i–iv) 20 μm and (v–viii) 2 μm .

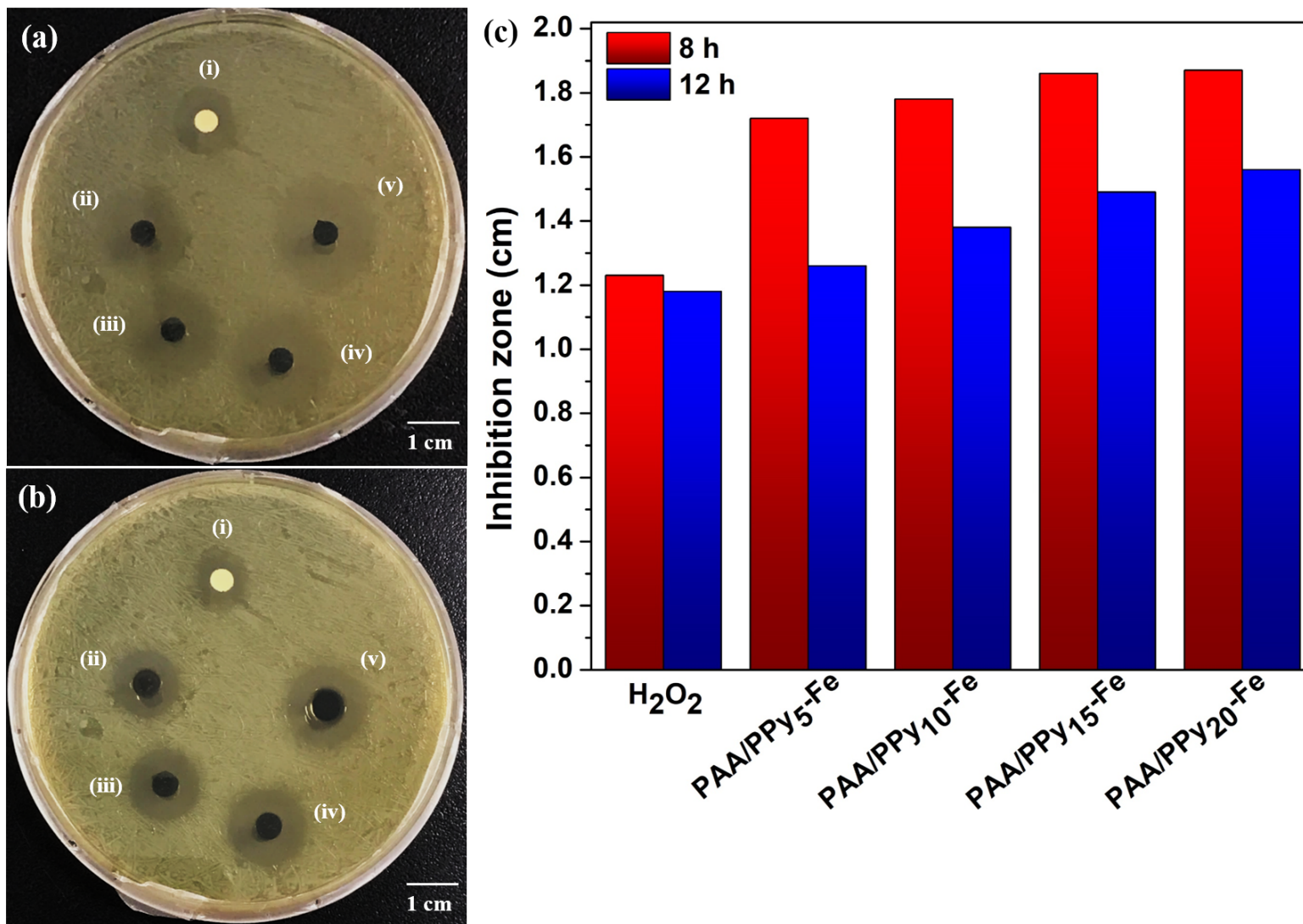


Figure 7 Antibacterial activity of hydrogels: (i) H_2O_2 ; (ii) PAA/PPy₅-Fe; (iii) PAA/PPy₁₀-Fe; (iv) PAA/PPy₁₅-Fe; and (v) PAA/PPy₂₀-Fe on *E. coli* bacteria incubated at 37°C for: (a) 8 h; (b) 12 h and (c) zone of inhibition of PAA/PPy-Fe

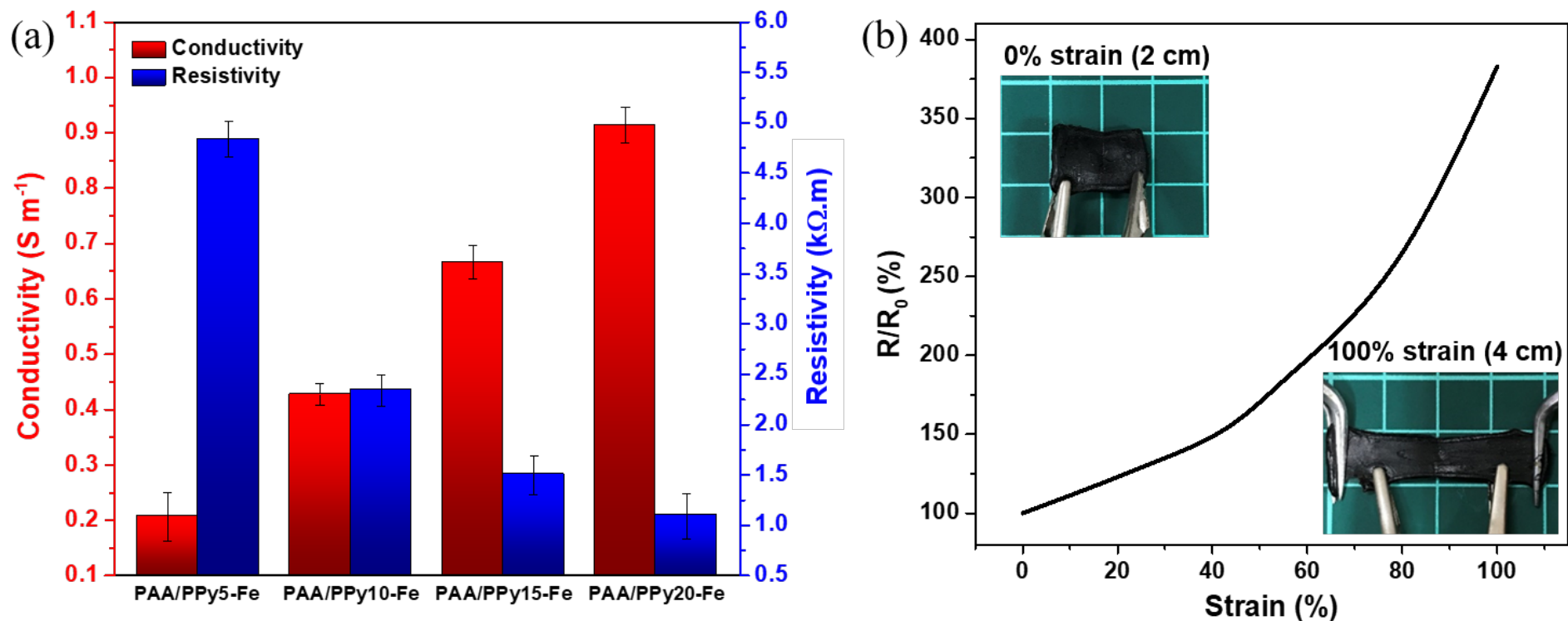


Figure 8 (a) the electroconductivity and resistivity of PAA/PPy-Fe hydrogels with various concentration of pyrrole and (b) resistance ratio-strain curve of PAA/PPy20-Fe hydrogel (the inserted photos are the strain at 0 and 100%).

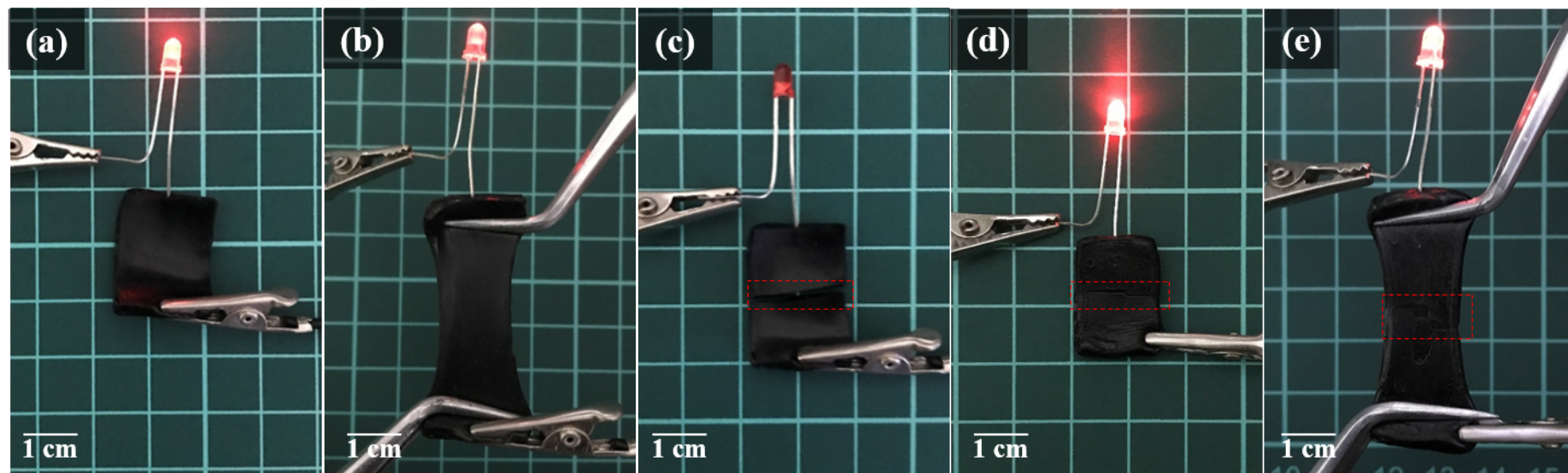


Figure 9. Photographs of PAA/PPy-Fe hydrogel conducting electricity in an electrical circuit, (a) original; (b) stretched; (c) cut-off; (d) healed; and (e) healed and stretched hydrogel.

Table 1. The elemental composition by EDX analysis of PAA/PPy-Fe composite hydrogels.

Hydrogels	Elements (atomic%)				Total (%)
	C	N	O	Fe	
PAA/PPy ₅ -Fe	55.86	1.01	41.98	1.15	100
PAA/PPy ₁₀ -Fe	47.09	9.32	40.77	2.82	
PAA/PPy ₁₅ -Fe	40.92	19.31	39.18	0.58	
PAA/PPy ₂₀ -Fe	40.49	20.67	38.01	0.83	

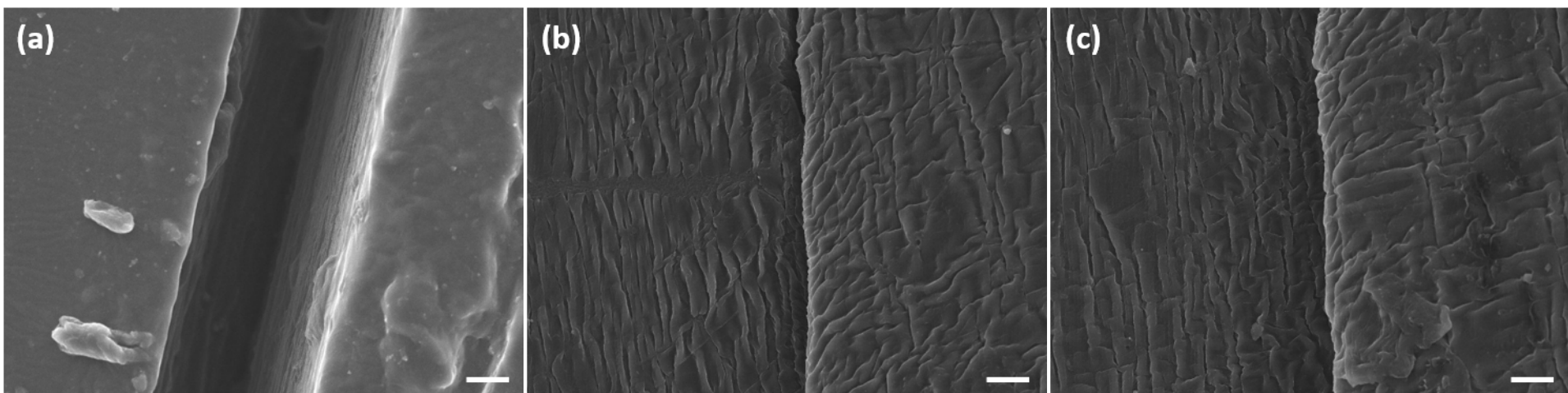
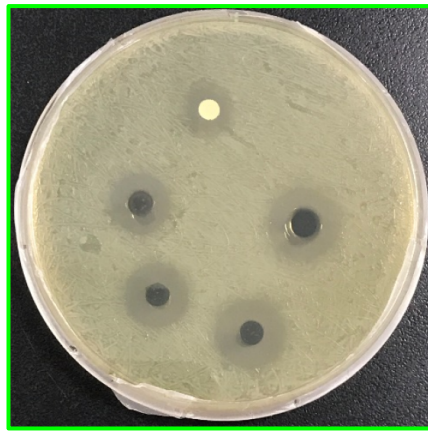
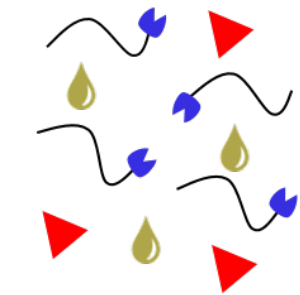
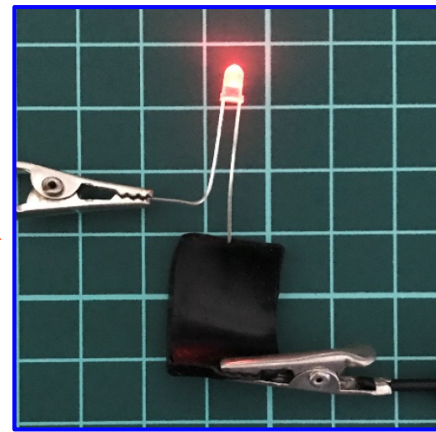


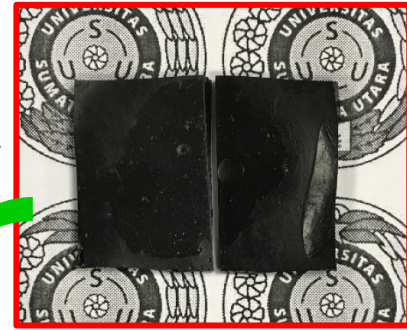
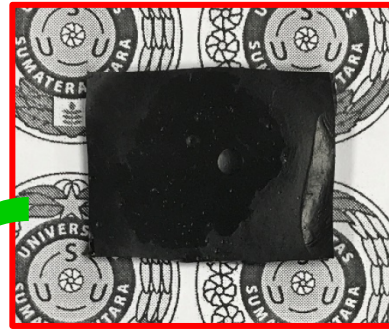
Figure 1S. SEM images of hydrogels during self-healing processes (a) cut-off, (b) healed at 37°C for (b) 3 h; and (c) 12 h at magnification of x1000 (scale bar 10 μm).



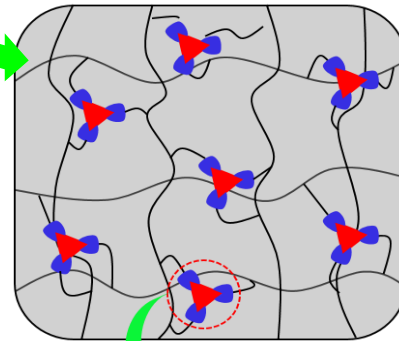
Antibacterial **Conductive**



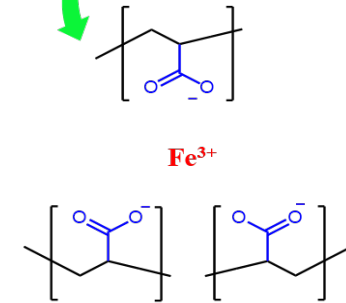
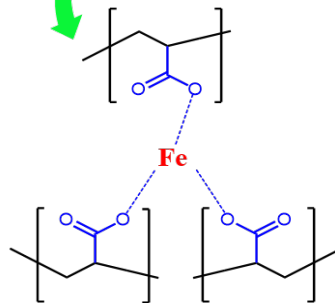
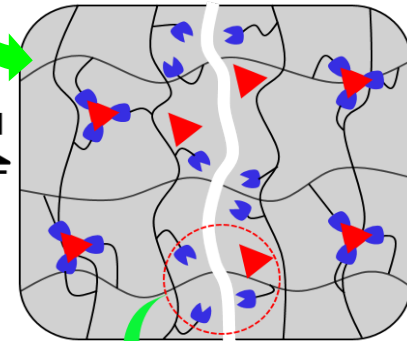
APS



- Acrylic acid
- Fe^{3+}
- Pyrrole



Damaged
Healing



Supporting Information for

Self-Healing Composite Hydrogel with Antibacterial and Reversible Restorability Conductive Properties

Mimpin Ginting^{a†*}, Subur P. Pasaribu^{b†}, Indra Masmur^a, Jamaran Kaban^a, and Hestina^c

^aDepartment of Chemistry, Faculty of Mathematics and Natural Sciences, Universitas Sumatera Utara, Medan-20155, Indonesia.

^bDepartment of Chemistry, Faculty of Mathematics and Natural Sciences, Mulawarman University, Samarinda-75123, Indonesia.

^cDepartment of Chemistry, Universitas Sari Mutiara Indonesia, Medan-20123, Indonesia.

†Ginting, M. and Pasaribu S. P. contributed equally to this work.

*Corresponding Author: Mimpin Ginting, Department of Chemistry, Faculty of Mathematics and Natural Sciences, Universitas Sumatera Utara, Medan-20155, Indonesia.

e-mail: mimpin.ginting@yahoo.com

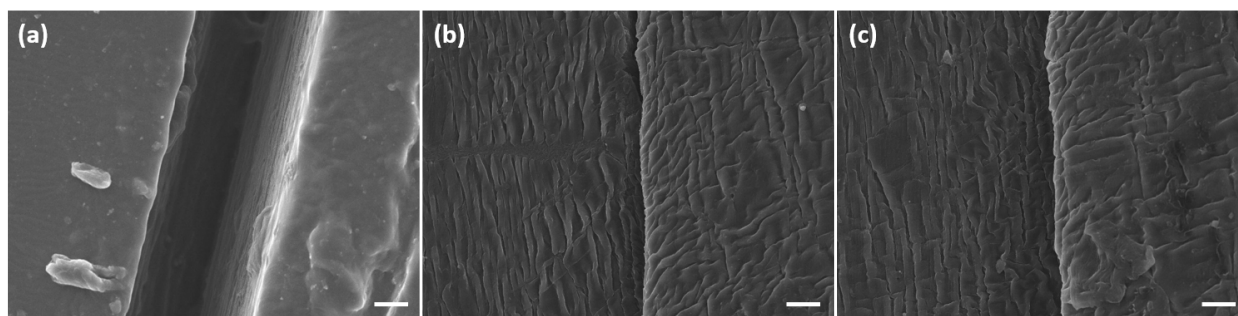


Fig. 1S. SEM images of hydrogels during self-healing processes (a) cut-off; healed at 37°C for (b) 6 h; and (c) 12 h at magnification of x1000 (scale bar 10 μ m).